Photovoltaic cells defects classification by means of Artificial Intelligence and electroluminescence images

Héctor Felipe Mateo-Romero[1[0000-0002-5569-3532]], Álvaro Pérez-Romero[2[0000-0002-4292-6640]], Luis Hernández-Callejo[1[0000-0002-8822-2948]], Sara Gallardo-Saavedra[1[0000-0002-2834-5591]], Víctor Alonso-Gómez[1[0000-0001-5107-4892]], José Ignacio Morales-Aragonés[1[0000-0002-9163-9357]], Alberto Redondo Plaza[1[0000-0002-2109-5614]] and Diego Fernández Martínez[1[0000-0003-1468-9083]]

[1] Universidad de Valladolid, Campus Universitario Duques de Soria, Soria 42004, Spain
[2] Universidad de Cantabria, Av. de los Castros, s/n, Santander 39005, Spain
thehfmr2011@gmail.com: H.F.M-R.; alvaro.pr470@gmail.com: A.P-R.; luis.hernandez.callejo@uva.es: L.H-C.; sara.gallardo@uva.es: S.G-S.; victor.alonso.gomez@uva.es: V.A-G.; ziguratt@coit.es: J.I.M-A.; alberredon@gmail.com: A.R.P.; diego-brivi@hotmail.com: D.F.M.

Abstract. More than half of the total renewable addictions correspond to solar photovoltaic (PV) energy. In a context with such an important impact of this resource, being able to produce reliable and safety energy is extremely important and operation and maintenance (O&M) of PV sites must be increasingly intelligent and advanced. The use of Artificial Intelligence (AI) for the defects identification, location and classification is very interesting, as PV plants are increasing in size and quantity. Inspection techniques in PV systems are diverse, and within them, electroluminescence (EL) inspection and current-voltage (I-V) curves are one of the most important. In this sense, this work presents a classifier of defects at the PV cell level, based on AI, EL images and cell I-V curves. To achieve this, it has been necessary to develop an instrument to measure the I-V curve at the cell level, used to label each of the PV cells. In order to determine the classification of cell defects, CNNs will be used. Results obtained have been satisfactory, and improvement is expected from a greater number of samples taken.

Keywords: photovoltaic cell defect, classifier, artificial intelligence, electroluminiscence.

1 Introduction

During the last years, global installation of renewable generation installations has significantly increased. In 2019, the last analyzed year in the Global Status Report [1], 201 GW of renewable power capacity were installed in the World, being 115 GW of Solar Photovoltaic (PV) capacity, which corresponds with more than 57% of the total renewable addictions.

In this context in which solar PV energy has such an important impact, being able to produce reliable and safety energy is extremely important. Ensuring energy production is a key factor in warranting plant profitability, and this has forced the design of increasingly intelligent and advanced Operation and Maintenance (O&M) strategies. Traditionally, different inspection techniques have been used in PV sites with the objective of detecting anomalies that reduce the system efficiency and can generate safety issues, as Infrared thermography inspections (IRT) [2], electroluminescence (EL) [3–5] or current-voltage (I-V) curves capturing [5, 6]. The development of new equipment and methodologies for its application in PV plants are necessary, and in this sense, research and industry are evolving rapidly [7]. The increased plant size has promoted the use of drones for the image capturing [8, 9], however the amount of data to process is unapproachable, requiring important human efforts and being very expensive and time-consuming.

The use of Artificial Intelligence (AI) for the defects identification, location and classification is very interesting. AI is already being applied in PV solar plants. However, its main application has being long focused on energy production forecasting issues. Authors in [10] develop a solution that provides the electricity production based on historical and current available solar radiation data in real-time. Some authors present a taxonomy study, which is a process to divide and classify the different forecasting methods, and the authors also present the trends in AI applied to generation forecasting in solar PV plants [11]. The use of artificial neural networks (ANN) has been successful in the last decade, some authors use ANN together with climatic variables to forecast generation in PV solar plants [12], while others use Support Vector Machine (SVM) together with an optimization of the internal parameters of the model [13]. ANN have also been used for other tasks, such as for the detection of problems in energy production, as is the case of work [14], where the authors use radial basis function (RBF) to detect this type of failure in production. A similar goal is sought in [15], where this time an SVM-based model is employed for describing a failure diagnosis method that uses a linear relation between the solar radiation and the power generation graphs. This research studies the following failure types: inverter failures, communication errors, sensor failures, junction box errors and junction box fire. The model classifies string and inverter failures. However, in actual PV plants each inverter can cover thousands of modules, and therefore important failures information can be lost in the classification [16].

In general, the application of AI technologies based on data-driven mechanisms helps to construct automatic fault classifiers and improves the efficiency and accuracy of faulty diagnoses [17]. A convolutional network, based on the analysis of the difference in the I-V curves of PV arrays under different failure states, capable of identifying not only a single failure (e.g., short circuit, partial shading, and abnormal aging) but also hybrid failures [17]. Authors in [18], authors investigate the effect of data augmentation techniques to increase the performance of our proposed convolutional neural network (CNNs) to classify anomalies between up to eleven different classes, in PV modules through thermographic images in an unbalanced dataset. This work is performed at the PV module level.

This work presents a classifier of defects at the PV cell level, based on AI, EL images and cell I-V curves. To achieve this, it has been necessary to make an instrument to measure the I-V curve at the cell level, used to label each of the PV cells. In order to determine the classification of cell defects, CNNs will be used. The document is structured as follows: section 2 presents the materials and methodology used, section 3 shows the results and discussion and section 4 deals the conclusions and future work.

2 Materials and methodology

This section is intended to explain the materials used, as well as the followed methodology to validate the classifier.

2.1 Materials

For this work, it has been necessary to develop special equipment and material. Firstly, regarding the PV devices, individual PV cells have been used. In this case, researchers have made the necessary welds to connect the required equipment, as it can be seen in Figure 1. One hundred PV cells have been used, which have subsequently been reused with artificial shadows, to have a greater number of measurements. Table 1 shows the basic electrical information of the PV cells used.

Figure 1. PV cell sample with welds already made.

Table 1. Information of PV cells.

PV cell parameter	PV cell parameter value
I_{SC} (A)	7.5
V_{OC} (V)	0.6
P_{MP} (W)	4.67

Once the PV cells were prepared as detailed before, it is necessary to obtain their individual I-V curves. To do this, it has been required to excite the PV cells, for which a LED board composed of 42 LEDs has been used with the following characteristics: OSRAM brand, 850 nm, 1 A forward current, 630 mW of radiant flux at 1 A and 100

microseconds, with a maximum temperature of 145 ºC. Figure 2 shows an image of the LED board. It has a diffuser screen to be able to homogenize the flow of light.

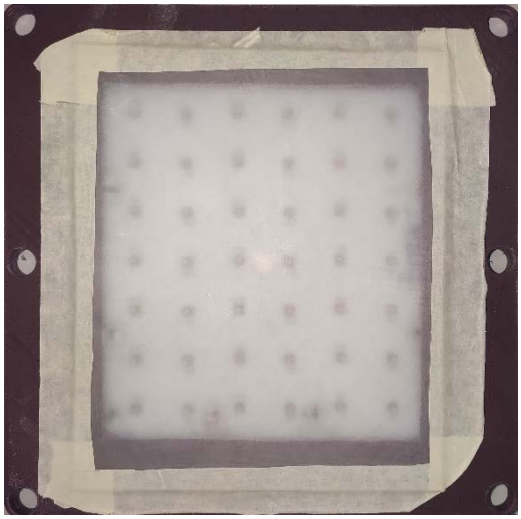

Figure 2. LED plate with diffuser mounted on support to take measurements.

Once the PV cells are illuminated with the LED board, the I-V curves are taken from an ingenious device developed by the authors, based on the charging and discharging of capacitors, and controlling the sweep by means of a simple microprocessor. This device is very versatile, since it allows to make the I-V curve from the second quadrant to the fourth quadrant through the first quadrant. However, for the presented research, the interest is only focused in the first quadrant.

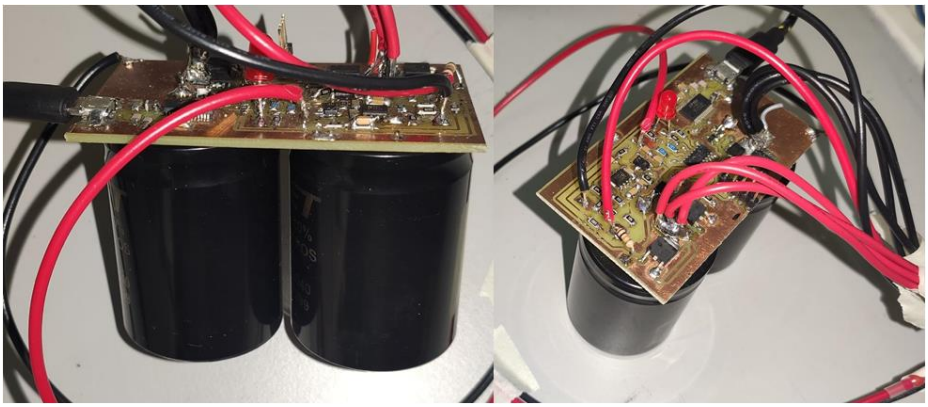

Figure 3. Device for drawing I-V curves at the PV cell level.

On the other hand, to be able to do EL, it is necessary to connect the PV cell to an external power source and to obtain the corresponding image. In this case, it is no needed to illuminate the PV cell (by means of an LED board). To be able to make the

capture, a special camera is necessary, specifically, it has been used an InGaAs camera, Hamamatsu brand and C12741-11 model.

Figure 4. InGaAs camera, Hamamatsu brand and C12741-11 model, for EL imaging.

Figure 5 a) shows a PV cell exposed to artificial irradiance to obtain its I-V curve, and Figure 5 b) shows the same PV cell subjected to inverse voltage to obtain its EL image.

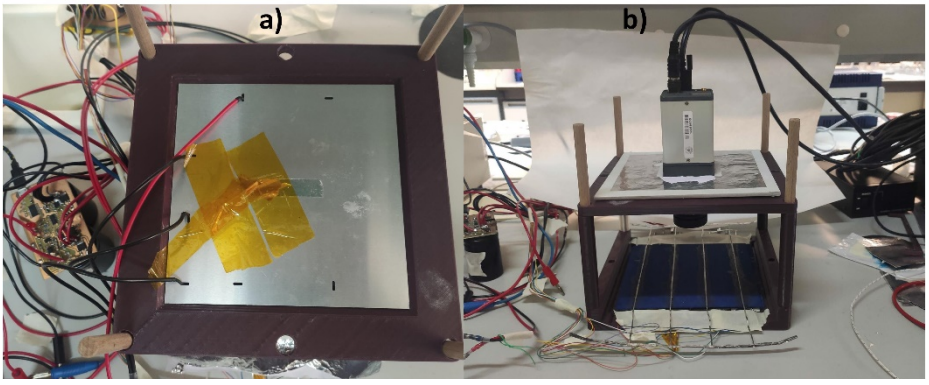

Figure 5. a) Obtaining I-V curve of PV cell; b) Obtaining EL image of PV cell.

2.2 Methodology

As already mentioned, the data was obtained manually, since the I-V curve of each of the cells of the data set was required, as well as their EL images. Therefore, none of the datasets that were in free repositories could be used. To carry out the EL images, an EL camera has been used, using different shades and irradiances to increase the amount of

data available in the final set. To obtain the I-V curve, the device built by the research team and previously presented has been used.

All images have had histogram adjustment done, making details and differences easier to see for the human eye, as well as for AI models. In order to be able to use the data of the I-V curve, the power values have been computed. Of all the values, only the highest value of each of the measurements will be taken into account. The power values will depend on the irradiance at which the measurement has been made, therefore, all measurements taken at the same irradiance will be processed. For this, the 5 highest power values will be chosen and the average will be made. In this way, authors will obtain a value that will represent the maximum power of a cell in good state. By choosing only the highest powers, the false information that the defective or shaded cells would provide will be ignored.

In order to have a greater number of samples, each of the measured cells has been subjected to partial shading, in order to repeat the measurements.

With the measurement of the absolute maximum power, authors will compute the relative power, calculating the proportion between the maximum power of each of the panels and the calculated power. This will give a continuous variable that will need to be divided into intervals if the problem is posed as a classification. The intervals should be decided in such a way that they allow the training to be carried out correctly and also the classes have a meaning in the context, that they are useful.

In Figure 6 it can be seen the histogram of the random variable and of the chosen classes. Class 0: PV cells in good condition (relative power > = 0.825); Class 1: PV cells in questionable condition (relative power < 0.825 and > = 0.725); Class 2: PV cells in poor condition (relative power < 0.725).

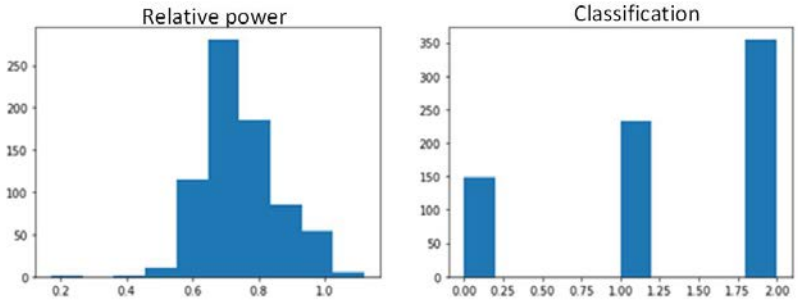

Figure 6. Relative power and classification of PV cells once the I-V curves have been made.

Once the information is available (I-V curves and EL images), it is necessary to use AI-based models to be able to train this models and to make the classifier. To resolve the classifier issue, it was decided to use an ANN-based architecture, specifically a CNNs, since it is a network that works very well with images. This is evident in the scientific literature. Figure 7 shows the architecture used and the relevant hyper-parameters.

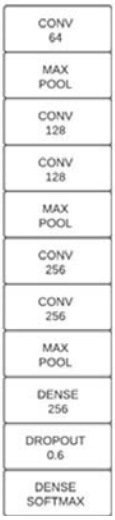

Hyper- parameters	Value
Learning rate	0.00005
Epochs	200
Batch size	16
Trigger function	ReLU
Output function	softmax
Dropout	Si
Optimizer	Adam
Función loss	Sparse categorical crossentropy
Metrics	accuracy

Figure 7. Optimized architecture and hyper-parameters.

The structure was chosen following a systematic procedure of trial and error. Different configurations were tried until the best results were found, a deeper network only resulted on over-fitting and shallow networks performed worse.

The hyperparameters were optimized following a similar approach. Different learning rates (0.05, 0.005, 0.0005, 0.00005, 0.000005) were compared. The one which the best performance was found to be 0.00005. This same principle was followed when setting the activation function: Relu was compared with Elu, Selu and Leaky Relu. The optimizer was chosen after comparing Adam with Nadam.

Other important feature of the system was the use of Data-Augmentation. An online data generation was used in the network training in other to improve its performance. The images went through limited rotations of less than 5 degrees and vertical or horizontal flips. The reason is that more intrusive modifications would not be real. Cells with big distortions would have a different IV curve. In each epoch new instances were generated choosing a new angle and flip.

Figure 8 shows the evolution of the accuracy and loss during the training and validation phases. In the accuracy graph, it can be seen how there is no difference between the train and validation sets, which implies that the network hardly experiences over fit. In the loss graph, an increase in over fit is observed from iteration 100, but at no point does it become considerable. The final network chosen will be that of iteration 195, which has a 90% in the validation set and a 0.5 in loss.

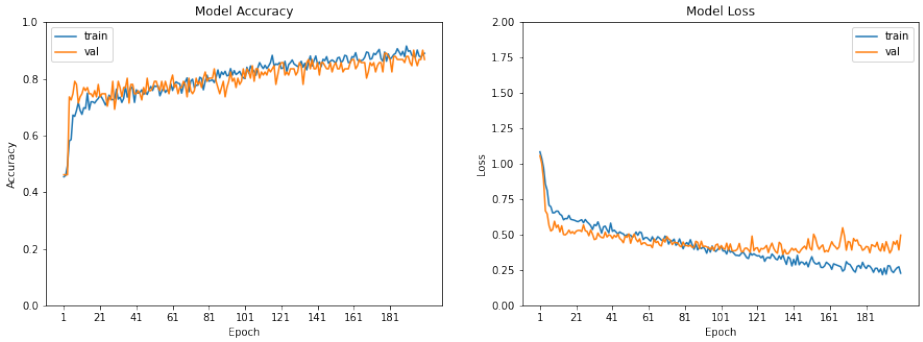

Figure 8. Evolution of accuracy and loss, for the training and validation phases.

3 Results and discussion

3.1 EL imaging and I-V curves

Figure 9 shows some EL images measured for this work. The images in the figure show the same PV cell, but with a different shade. The figure at the top left shows a PV cell without a shadow, but with a failure defect in the middle of it. The rest EL images, show the same PV cell with different added artificial shadows.

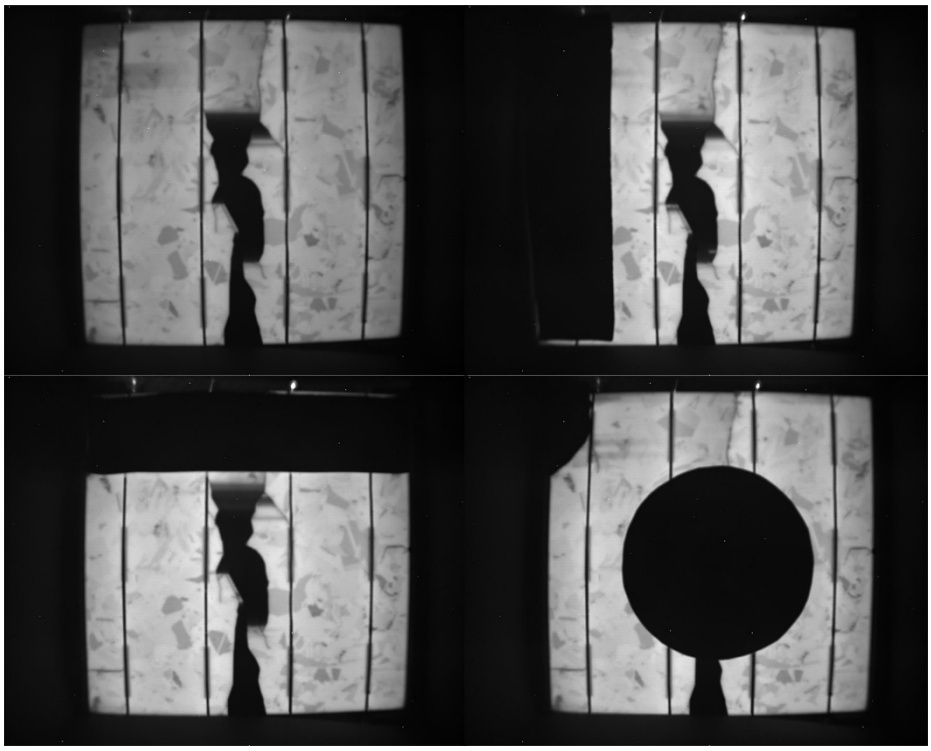

Figure 9. EL images of a PV cell with different artificial shadows.

Figure 10 shows the measurements of the I-V curves of a specific PV cell. The different curves represent the I-V curve at different irradiances levels and/or with artificial shadows. The figure also shows the P-V curves of the PV cell.

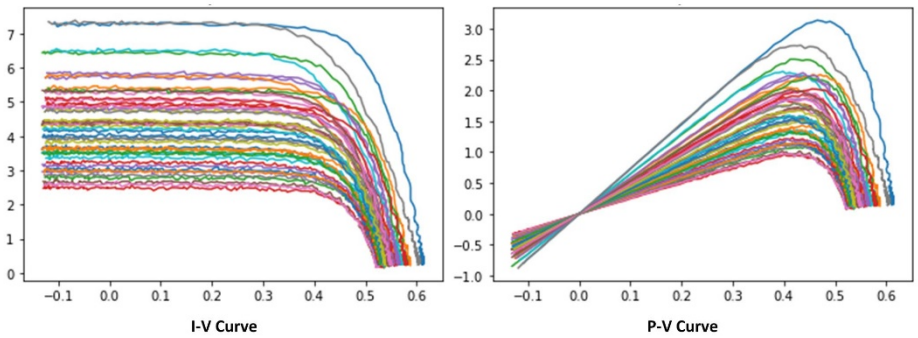

Figure 10. I-V curves of a specific PV cell and P-V curves.

3.2 CNNs

With the available data, the CNNs has been trained and its results have been obtained, after the validation phase.

In Figure 11, it can be seen how the behavior in the non-training data set is similar to the validation one, reaching 87% precision, a very high behavior and very similar to that obtained in the validation during the training phase. It can be seen how the CNNs perfectly distinguishes classes 0 and 2, with only one instance in which an error occurs, which indicates that the model differentiates PV cells in good condition from PV cells in poor condition. For class 1, its behavior can be improved, since it has more difficulties to classify this class well, although it still gives good results. The inclusion of data augmentation improved the performance of the model.

Validation set

Confusion matrix

```
[[20  0  0]
 [ 1 24  4]
 [ 0  4 38]]
```

Classification report

	precision	recall	f1-score	support
0	0.95	1.00	0.98	20
1	0.86	0.83	0.84	29
2	0.90	0.90	0.90	42
accuracy			0.90	91
macro avg	0.90	0.91	0.91	91
weighted avg	0.90	0.90	0.90	91

Final set

Confusion matrix

```
[[18  1  0]
 [ 1 26  1]
 [ 1  7 31]]
```

Classification report

	precision	recall	f1-score	support
0	0.90	0.95	0.92	19
1	0.76	0.93	0.84	28
2	0.97	0.79	0.87	39
accuracy			0.87	86
macro avg	0.88	0.89	0.88	86
weighted avg	0.89	0.87	0.87	86

Figure 11. Results of the CNNs.

4 Conclusions and future work

The work has presented a classifier of defects in PV cells, based on AI and from EL images. For the perfect classification, it was necessary to use the I-V curve of each of the PV cells. For this, it has been necessary to make an instrument to measure the I-V curve at the cell level, which has served to label each of the PV cells. A CNNs has been used, and the results obtained have been satisfactory, and improvement is expected from a greater number of samples taken.

The researchers will expand the data set manually and using techniques to generate synthetic data as Generative Adversative Neural Networks (GANN), and will try another type of PV cell. In addition, the intention is to classify the defects of complete PV modules.

Acknowledgments

The authors thank the CYTED Thematic Network “INTELLIGENT CITIES FULLY INTEGRAL, EFFICIENT AND SUSTAINABLE (CITIES)” nº 518RT0558.

References

1. REN21 Secretariat: Renewables 2020 Global Status Report. (2020).
2. Jordan, D.C., Silverman, T.J., Wohlgemuth, J.H., Kurtz, S.R., VanSant, K.T.: Photovoltaic failure and degradation modes. Prog. Photovoltaics Res. Appl. 25, 318–326 (2017). https://doi.org/10.1002/pip.2866.
3. Kendig, D., Alers, G.B., Shakouri, A.: Characterization of defects in photovoltaics using thermoreflectance and electroluminescence imaging. Conf. Rec. IEEE Photovolt. Spec. Conf. 1733–1736 (2010). https://doi.org/10.1109/PVSC.2010.5616126.
4. Fuyuki, T., Kitiyanan, A.: Photographic diagnosis of crystalline silicon solar cells utilizing electroluminescence. Appl. Phys. A Mater. Sci. Process. 96, 189–196 (2009). https://doi.org/10.1007/s00339-008-4986-0.
5. Gallardo-Saavedra, S., Hernández-Callejo, L., Alonso-García, M. del C., Santos, J.D., Morales-Aragonés, J.I., Alonso-Gómez, V., Moretón-Fernández, Á., González-Rebollo, M.Á., Martínez-Sacristán, O.: Nondestructive characterization of solar PV cells defects by means of electroluminescence, infrared thermography, I-V curves and visual tests: experimental study and comparison. Energy. 205, 1–13 (2020). https://doi.org/https://doi.org/10.1016/j.energy.2020.117930.
6. Blakesley, J.C., Castro, F.A., Koutsourakis, G., Laudani, A., Lozito, G.M., Riganti Fulginei, F.: Towards non-destructive individual cell I-V characteristic curve extraction from photovoltaic module measurements. Sol. Energy. 202, 342–357 (2020). https://doi.org/10.1016/j.solener.2020.03.082.
7. Hernández-Callejo, L., Gallardo-Saavedra, S., Alonso-Gómez, V.: A review of photovoltaic systems: Design, operation and maintenance. Sol. Energy. 188, 426–440 (2019). https://doi.org/10.1016/j.solener.2019.06.017.
8. Gallardo-Saavedra, S., Hernández-Callejo, L., Duque-Perez, O.: Technological review of the instrumentation used in aerial thermographic inspection of photovoltaic plants. Renew. Sustain. Energy Rev. 93, 566–579 (2018). https://doi.org/10.1016/j.rser.2018.05.027.
9. Gallardo-Saavedra, S., Hernandez-Callejo, L., Duque-Perez, O.: Image Resolution Influence in Aerial Thermographic Inspections of Photovoltaic Plants. IEEE Trans. Ind. Informatics. 14, 5678–5686 (2018). https://doi.org/10.1109/TII.2018.2865403.
10. Gligor, A., Dumitru, C.D., Grif, H.S.: Artificial intelligence solution for managing a photovoltaic energy production unit. Procedia Manuf. 22, 626–633 (2018). https://doi.org/10.1016/j.promfg.2018.03.091.
11. Wang, H., Liu, Y., Zhou, B., Li, C., Cao, G., Voropai, N., Barakhtenko, E.: Taxonomy research of artificial intelligence for deterministic solar power forecasting. Energy Convers. Manag. 214, 112909 (2020). https://doi.org/10.1016/j.enconman.2020.112909.
12. Kayri, I., Gencoglu, M.T.: Predicting power production from a photovoltaic panel through artificial neural networks using atmospheric indicators. Neural Comput. Appl. 31, 3573–3586 (2019). https://doi.org/10.1007/s00521-017-3271-6.
13. Li, L.L., Wen, S.Y., Tseng, M.L., Chiu, A.S.F.: Photovoltaic array prediction on short-term output power method in Centralized power generation system. Ann. Oper. Res. 290, 243–263 (2020). https://doi.org/10.1007/s10479-018-2879-y.

14. Hussain, M., Dhimish, M., Titarenko, S., Mather, P.: Artificial neural network based photovoltaic fault detection algorithm integrating two bi-directional input parameters. Renew. Energy. 155, 1272–1292 (2020). https://doi.org/10.1016/j.renene.2020.04.023.
15. Cho, K.H., Jo, H.C., Kim, E. sang, Park, H.A., Park, J.H.: Failure Diagnosis Method of Photovoltaic Generator Using Support Vector Machine. J. Electr. Eng. Technol. 15, 1669–1680 (2020). https://doi.org/10.1007/s42835-020-00430-9.
16. Pérez-Romero, Á., Mateo-Romero, H.F., Gallardo-Saavedra, S., Alonso-Gómez, V., Alonso-García, M. del C., Hernández-Callejo, L.: Evaluation of Artificial Intelligence-Based Models for Classifying Defective Photovoltaic Cells. Appl. Sci. 11, 4226 (2021). https://doi.org/10.3390/app11094226.
17. Gao, W., Wai, R.J.: A Novel Fault Identification Method for Photovoltaic Array via Convolutional Neural Network and Residual Gated Recurrent Unit. IEEE Access. 8, 159493–159510 (2020). https://doi.org/10.1109/ACCESS.2020.3020296.
18. Fonseca Alves, R.H., Deus Júnior, G.A. de, Marra, E.G., Lemos, R.P.: Automatic fault classification in photovoltaic modules using Convolutional Neural Networks. Renew. Energy. 179, 502–516 (2021). https://doi.org/10.1016/j.renene.2021.07.070.